



## **Method for direct measurements of luminescent coupling efficiency in concentrator MJ SCs**

M. Z. Shvarts, M. A. Mintairov, V. M. Emelyanov, V. V. Evstropov, V. M. Lantratov, and N. Kh. Timoshina

Citation: [AIP Conference Proceedings](#) **1556**, 147 (2013); doi: 10.1063/1.4822219

View online: <http://dx.doi.org/10.1063/1.4822219>

View Table of Contents: <http://scitation.aip.org/content/aip/proceeding/aipcp/1556?ver=pdfcov>

Published by the [AIP Publishing](#)

---



recombination  $U_d$  the contribution into the diffusion component of current is given by band-to-band radiation recombination (luminescence)  $L$  (Figure 1).

The following set of equations gives in a parametric form the dependence of the  $L$  on the “internal” current density  $J_L$ :

$$\begin{cases} J_L = J_d + J_r = J_{0d} \exp\left(\frac{V_j}{kT/q}\right) + J_{0r} \exp\left(\frac{V_j}{2kT/q}\right) \\ L = L_{0d} \exp\left(\frac{V_j}{kT/q}\right) \\ J_d = qL + qU_d \\ J_{0d} = qL_{0d} + qU_{0d} \end{cases} \quad (1)$$

where  $V_j$  is voltage on the p-n junction (difference between the quasi-Fermi levels inside the p-n junction space charge region;  $J_L$  is the “internal” current density, i.e. the current flowing through the emitting p-n junction and causing electroluminescence;  $L$  is the quantum luminosity (luminescence) characterizing the number of photons irradiated per unit time from unit area in the half-space;  $q$  is the electron charge;  $kT$  is the thermal energy;  $J_{0d}, J_{0r}, L_{0d}, U_{0d}$  are the preexponents.

The “transfer” function in the proposed method is defined as:

$$\gamma(J_L) = Q_L(J_L) \cdot p \cdot Q_{ph} \quad (2)$$

where  $\gamma$  is transfer (coupling) yield,  $Q_L = qL/J_L$  is the  $WB$  p-n junction quantum yield of EL (in half space);  $p$  is the transmittance coefficient of layers between p-n junction;  $Q_{ph}$  is the narrow bandgap p-n junction quantum yield of the photoresponse.

Motivation for introducing the  $\gamma$  and two proportionality coefficients  $p$  and  $Q_{ph}$  will be considered in the next paragraph.

So, if in the system (1) instead of luminosity  $L$  entering  $\gamma$  and eliminating  $\exp\left(\frac{V_j}{kT/q}\right)$ , the function  $\gamma(J_L)$  (exact inverse function) takes the form:

$$J_L = J_{rd} \frac{\gamma/\gamma_s}{(1 - \gamma/\gamma_s)^2}, \quad (3)$$

where  $J_{rd} = J_{0r}^2/J_{0d}$  is a conditional current boundary between the recombination and diffusion sections of the dark I-V characteristic for the radiating p-n junction;  $\gamma_s = Q_{ph} \cdot p \cdot Q_s$  is the limiting (saturated) value for function  $\gamma(J_L)$ , in which  $Q_s = qL_{0d}/J_{0d}$  is

the limiting quantum yield of the electroluminescence into the half-space on the diffusion portion of the dark I-V characteristic.

## LUMINESCENCE INDUCED CURRENT IN NB P-N JUNCTION

Quantum irradiance  $E$  of the  $NB$  p-n junction is proportional to luminosity:  $E = p \cdot L$ , and the additional current induced in this subcell at absorption of luminescent radiation is also proportional to  $E$ :

$$\Delta J_N = Q_{ph} \cdot qE, \quad (4)$$

Since the luminosity  $L$  is related to the “internal” current  $J_L$  through the EL quantum yield  $Q_L(J_L)$ , the current increment  $\Delta J_N$  and “internal” current  $J_L$  are coupled by the function:

$$\gamma(J_L) = \Delta J_N / J_L. \quad (5)$$

From the equivalent circuit (see Figure 1) for each of nodes “a”, “b”, “c” of electrical circuit the following current balances are:

$$J_w = J_L + J, \quad J_N = J + J_D, \quad J_N = J_{N0} + \Delta J_N$$

Then it follows from equation (5):

$$\gamma(J_L) = \frac{J_N - J_{N0}}{J_w - J} = \frac{J_N - J_{N0}}{J_w - J_N + J_D} \quad (6)$$

In the short circuit regime the following equalities are:  $J = J_N$ ,  $J_D = 0$ , then (6) could be rewritten as:

$$\gamma(J_L) = \frac{J_N - J_{N0}}{J_w - J_N} \quad (7)$$

Physical meaning embodied in the  $\gamma(J_L)$  is fully consistent with the definition of “quantum efficiency of the luminescent coupling”, proposed in [15], and parameter  $\gamma_s$  is equivalent to the «coupling efficiency» in [8]. The variable quantity  $\gamma$  is associated with  $X_{LC}$  («luminescent coupling factor») from [10] via the relationship  $\gamma = X_{LC}/(1 - X_{LC})$ .

## EXPERIMENTAL DETERMINATION OF FUNCTION $\gamma(J_L)$

In this section the two-stage experiment for obtaining  $\gamma(J_L)$  for any pair of subcells being in a direct optoelectronic contact is presented.

In the first experiment, the  $J_{SC}$  is always equal to the current of  $WB$  subcell  $J_{SC} = J_w$  (at the condition of

$R_s < V_{oc} / J_w$ ). The relationships between the irradiances for subcells are preset in such a way that  $J_w$  is much lower than  $J_N$ , and also lower than currents generated in any subcells, which have not been chosen as a pair for the analysis. Further, in increasing the irradiance  $E_w$  in the spectral sensitivity range of the *WB* subcell, the rise of  $J_w$  is recorded.

In the second experiment, the initial ratios of the irradiances are adjusted so that the currents generated in any other (not included into the pair of interest) subcells would be greater than  $J_w$  and  $J_N$ , while the  $J_w \geq J_N$ . Then, to ensure the rise of  $J_w$  the irradiance have been increased in the same way as in the previous case, and the current  $J_{SC} = J_N = \Delta J_N$  is registered ( $J_{N0} = 0$  since external illumination within spectral range of the *NB* subcell is absent in presented below practical case and only current induced by EL irradiation is accounted).

So for each irradiations  $E_w$  the two values  $J_w$  and  $J_N$  are obtained and the sought-for dependence of the transfer (coupling) function  $\gamma(J_L)$  is calculated.

## TECHNIQUE AND PROCEDURE FOR MEASUREMENT

In carrying out experiments, a dual-lamp sunlight simulator has been used with a system for positioning interference filters and two movable light shields (Figure 2). The radiation flux from two pulsed lamps located close to each other and operating synchronously passes through blue, red and IR interference filters and creating conditions for selective action on GaInP, GaAs and Ge subcells of a 3J SC. The simulator design allows setting the filters in different combinations. For the light action on the GaInP and GaAs subcells, blue ( $\lambda=300-650$  nm) and red ( $\lambda=690-900$  nm) filters were used, and at operation with the GaInP and Ge subcells – blue and IR ( $\lambda>900$  nm) ones. Introducing IR glass narrow strips between the blue and red filters ensured simultaneous action on a 3J SC in three spectral ranges. In increasing number of IR glass strips, a step-like enrichment of the IR irradiation was performed, i.e. irradiation level rise for Ge subcell is realized.

A set of the light-filters can be moved with respect to the light window. At that, the introducing one filter into the light flux at simultaneous taking-off of another one. So, the radiation spectrum is enriched in the blue or red wavelength ranges (Figure 2, in shifting filters to the right or left to obtain conditions for excess current in the top or middle subcells, correspondingly). A smooth regulation of the irradiance levels in the

range of subcells sensitivity was fulfilled at overlapping a part of the light-filters' apertures by movable shields. Irradiance levels as high as 500X were possible to be achieved for each of subcells of 3J SC in decreasing illuminator-SC distance with keeping good uniformity of irradiance on SC. It is obvious that, in accordance with the sequence in introducing the radiation of corresponding spectral range into the general light flux and with the color balance "blue/red/IR" established at each shield position, a 3J SC can be "configured" by values of the generated current in the subcells in any of the following versions:  $I_{top} > I_{mid} > I_{bot}$ ,  $I_{bot} > I_{top} > I_{mid}$ ,  $I_{bot} > I_{mid} > I_{top}$  and so on.

Recording of the SC I-V characteristic was being carried out during the flat part of the 1msec light pulse. Taking into account a probable current flow through the Ge subcell at a reverse voltage bias in recording the I-V characteristic, in scanning in the voltage range of  $-4 \div +3.5V$ , it was allowed registering the photocurrent values at once for two subcells being in the conditions of strong current mismatch. The light flux density increase/decrease is ensured by a smooth shift of opaque shields with respect to the installed filters, and the irradiance level ( $E$ ) in each spectral range obtained for selected shield position appears to be strictly proportional to the corresponding filter aperture width. Thus, in carrying out experiments, a direct monitoring of the irradiance level in each spectral range is not obligatory. It is just enough to control the corresponding light filter aperture width.

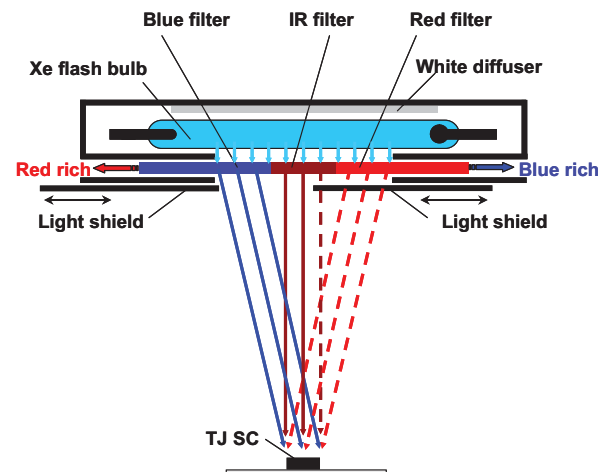


**FIGURE 2.** Optical scheme of pulsed solar simulator. By colored arrows the possible directions of filter movement are indicated. Right shield is shown in a position then IR light flux intended for Ge subcell is slightly reduced, but red light for GaAs subcell is fully blocked.

## RESULTS AND DISCUSSION

Construction of the transfer (coupling) function for the pairs of GaInP-GaAs and GaAs-Ge subcells being analyzed was carried out on the basis of experimental data (Figure 3) recorded at the two-stage measurement procedure described above. Since  $J_L = J_W - J_N$ , substituting for  $J_W$ ,  $J_N$  and  $J_{N0} = 0$  into the (7) the dependence  $\gamma(J_L)$  was obtained and later on approximated by (3), where the sought-for values  $J_{rd}$  and  $\gamma_s$  were used as fit parameters (Figure 4).

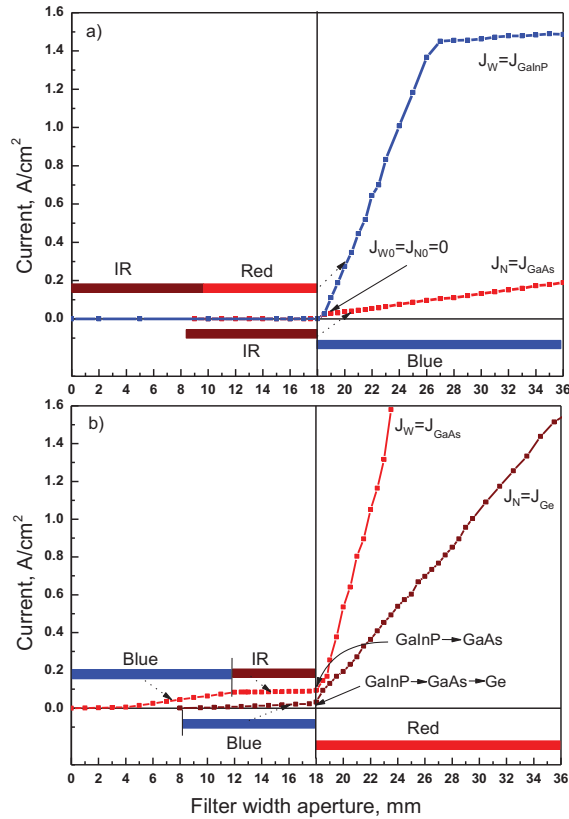


**FIGURE 3.** Dependencies of the subcells photocurrents of on the light pumping level for cell pairs: a) GaInP-GaAs, b) GaAs-Ge. The colored rectangles show the ranges of openings of the filters transmitting light within the sensitivity ranges of subcells: blue – GaInP, red – GaAs, brown – Ge.

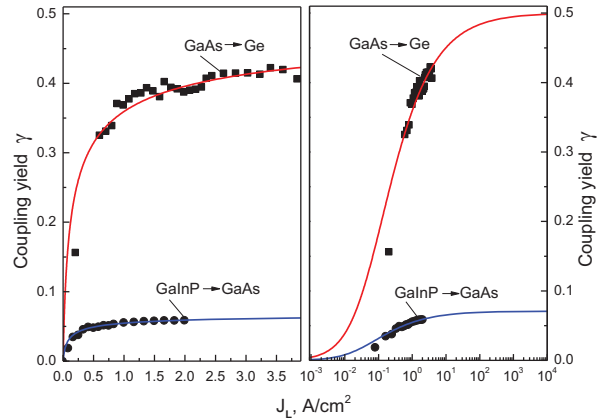


**FIGURE 4.** Transfer function  $\gamma(J_L)$  for the GaInP-GaAs and GaAs-Ge subcells pairs in linear (on the left) and semi-logarithmic (on the right) scales: dots are the experimental data, solid lines are the calculated by formula (3) data.

It is clear that, for the pair GaInP-GaAs the luminescent induced current in GaAs can, at high irradiances, achieve 7% (coupling yield) of the GaInP “internal” current. The obtained value of  $J_{rd} = 7 \cdot 10^{-2}$  A/cm<sup>2</sup> corresponds to those from [18].

For the GaAs-Ge pair, the fit parameters are  $\gamma_s = 0.5$  и  $J_{rd} = 1.1 \cdot 10^{-1}$  A/cm<sup>2</sup>, which also correspond to those from [18]. It should be noted that coupling yield rise for the GaAs-Ge pair almost stops (within an accuracy of up to 5%) at the current densities of higher than 100 A/cm<sup>2</sup>. However, so high photocurrents are practically not achievable for SCs operating in practical systems with sunlight concentrators. At the same time the obtained  $\gamma(J_L)$  dependencies allow determining the luminescent contribution into the generated current at low levels of the photocurrent mismatch between subcells.

## ACKNOWLEDGMENTS

The authors wish to thank Prof. V. Andreev for support of this work. Special thanks to N. A. Kalyuzhnyy and S. A. Mintairov for SCs development. Support for this work partly comes from the RFBR (Grants 12-08-01019-a, 12-08-01034-a, 13-08-00534-a) and the Ministry of education and science of Russia (Grant No 8075 dated 20.07.2012).

## REFERENCES

1. M.A.Green, et al., “Solar cell efficiency tables (version 41)”, Prog. PV: Res. Appl., 2013, 21, pp.1–11.
2. R. R. King, et al., Prog. PV: Res. Appl., 2012, 20, pp. 801–815
3. M. Wiemer, et al., Proc. of SPIE 2011, vol. 8108, p. 810804-1 - 810804-5.
4. H. Yoon, et al., 3<sup>rd</sup> WCPEC, 2003, vol.1, pp.745–748.
5. C. Baur, et al., Appl. Phys. Lett., vol. 90, pp. 192109-1–192109-3, 2007.
6. V.D.Rumyantsev, et al., Proc. of the CPV-6, 2010, Freiburg, Germany, pp. 20-23.
7. S. H. Lim, et al., Prog. PV: Res. Appl., vol. 10, pp. 1215–1221, 2011.
8. M. A. Steiner and J. F. Geisz, Appl. Phys. Lett., vol. 100, no. 25, pp. 251106-1–251106-5, 2012.
9. K. H. Lee, et al., *IEEE J. Photovoltaics*, vol. 2, no. 1, pp. 68–74, Jan. 2012.
10. D. Derkacs, et al., *IEEE J. Photovoltaics*, vol. 3, no. 1, pp. 520–527, Jan. 2012.
11. M. A. Steiner, et al., *IEEE J. Photovoltaics*, vol. 3, no. 2, pp. 879-887, April 2013.
12. J.-J. Li, et al., *IEEE J. Photovoltaic*, vol. 1, no. 2, pp. 225–230, Oct. 2011.
13. J.-J. Li, Y.-H. Zhang, *IEEE J. Photovoltaics*, vol. 3, no. 1, pp. 364-369, January 2013.
14. M. A. Steiner, et al., *IEEE J. Photovoltaics*, vol. 2, no. 4, pp. 424–433, Oct. 2012.
15. Charles et al., , 37<sup>th</sup> IEEE PVSC, 2011, pp. 452-453
16. W. Shockley, Bell System Tech. J., 28 (3), 1949, pp. 435.-489.
17. C. T. Sah, R.N.Noyce, W.Shockley, Proc. IRE, v.45, issue 9, pp.1228-1243
18. V.S. Kalinovsky, et al., 23<sup>rd</sup> EUPVSEC, Valencia, Spain, 2008, pp. 773-776.